



Published in final edited form as:

Clin Cancer Res. 2012 September 15; 18(18): 4931–4941. doi:10.1158/1078-0432.CCR-12-0697.

Copper chelation enhances anti-tumor efficacy and systemic delivery of oncolytic HSV

Ji Young Yoo¹, Jason Pradarelli^{1,2}, Amy Haseley¹, Jeffrey Wojton¹, Azeem Kaka^{1,5}, Anna Bratasz^{3,4}, Christopher Alvarez-Breckenridge^{1,6}, Jun Yu⁷, Kimerly Powell^{3,4}, Andrew Mazar⁷, Theodoros N Teknos⁸, E. Antonio Chiocca¹, Joseph C. Glorioso⁹, Matthew Old⁷, and Balveen Kaur¹

¹Dardinger Laboratory for Neuro-oncology and Neurosciences; ¹Department of Neurological Surgery, Northwestern University, 2145 Sheridan Rd. Evanston IL 60208

²Biomedical Science Major, Northwestern University, 2145 Sheridan Rd. Evanston IL 60208

³Small Animal Imaging Shared Resources, Northwestern University, 2145 Sheridan Rd. Evanston IL 60208

⁴Department of Biomedical Informatics, Northwestern University, 2145 Sheridan Rd. Evanston IL 60208

⁵Department of Otolaryngology, Northwestern University, 2145 Sheridan Rd. Evanston IL 60208

⁶Medical Scientist Training Program, Northwestern University, 2145 Sheridan Rd. Evanston IL 60208

⁷Chemistry of Life Processes Institute and Robert H. Lurie Comprehensive Cancer Center, Northwestern University, 2145 Sheridan Rd. Evanston IL 60208

⁸Department of Otolaryngology Head and Neck Surgery and James Comprehensive Cancer Center, The Ohio State University Wexner Medical center, Columbus, OH, 43210

⁹Department of Microbiology and Molecular Genetics, University of Pittsburgh, School of Medicine, Pittsburgh, Pennsylvania 15219

Abstract

Purpose—Copper in serum supports angiogenesis and inhibits replication of wild type HSV-1. Copper chelation is currently being investigated as an anti-angiogenic and anti-neoplastic agent in patients diagnosed with cancer. Herpes simplex virus derived oncolytic viruses (oHSVs) are being evaluated for safety and efficacy in patients, but several host barriers limit their efficacy. Here, we tested if copper inhibits oHSV infection and replication and if copper chelation would augment therapeutic efficacy of oHSV.

Experimental Design—Subcutaneous and intracranial tumor bearing mice were treated with oHSV ± ATN-224 to evaluate tumor burden and survival. Virus replication and cell killing was measured in the presence or absence of the copper chelating agent ATN-224 and in the presence or absence of copper in vitro. Micro-vessel density and changes in perfusion were evaluated by immuno-histochemistry and DCE-MRI. Serum stability of oHSV was measured in mice fed with

* Address correspondence and reprint requests to Dr. Balveen Kaur, Department of Neurological Surgery, Dardinger Laboratory for Neuro-oncology and Neurosciences, The Ohio State University, 385-D OSUCCC, 410 West 12th Avenue, Columbus, OH 43210. Tel: 614-292-3984, Fax: 614-688-4882, balveen.kaur@osumc.edu.

Conflict of Interest: None

ATN-224. Tumor bearing mice were injected intravenously with oHSV; tumor burden and amount of virus in tumor tissue was evaluated.

Results—Combination of systemic ATN-224 and oHSV significantly reduced tumor growth and prolonged animal survival. Immunohistochemistry and DCE-MRI imaging confirmed that ATN-224 reduced oHSV-induced blood vessel density and vascular leakage. Copper at physiologically relevant concentrations inhibited oHSV replication and glioma cell killing and this effect was rescued by ATN-224. ATN-224 increased serum stability of oHSV and enhanced the efficacy of systemic delivery.

Conclusion—This study shows that combining ATN-224 with oHSV, significantly increased serum stability of oHSV and greatly enhanced its replication and antitumor efficacy.

Keywords

Glioblastoma (GBM); Oncolytic Virus (OV); Herpes Simplex Virus-1 (HSV-1); ATN-224; Copper ions (Copper)

Introduction

Oncolytic virus therapy is emerging as a novel strategy for the treatment of patients with a diverse range of cancers, including glioma (1). Oncolytic viruses derived from Herpes Simplex Virus-1 (oHSVs) have been tested in several clinical trials for the treatment of malignant glioma and have shown low toxicity with encouraging indications of efficacy (2). However, efficient oncolysis *in vivo* is impeded by several tumoral and/or host barriers, and an effort to understand and overcome these barriers remains critically important to improve therapeutic efficacy (3).

Changes in tumor microenvironment following viral oncolysis result in increased angiogenesis in residual tumor after viral clearance (4–5). Consistent with this, therapy which combines oHSV with anti-angiogenic agents has been shown to improve anti-tumor efficacy significantly (5–11).

Copper functions as an important co-factor for several angiogenic growth factors, including VEGF and angiogenin, and is also required for the secretion of several angiogenic factors by tumor cells (12–13). An elevation of serum copper levels found in many human tumors correlates with an increased tumor burden and a worsened prognosis (14). Apart from supporting angiogenesis, copper found in serum has been shown to inhibit wild-type HSV infection and its topical use is currently being evaluated as an anti-herpetic agent in patients with herpes skin lesions (15–17).

Tetrathiomolybdate (TM) is a first generation copper chelator that creates a complex with copper and serum albumin, effectively restricting cellular uptake of copper. Treatment of cancer cell lines with TM has shown a reduction in the levels of pro-angiogenic and pro-inflammatory mediators and a significant antitumor efficacy *in vivo* (18–20). Copper chelation is currently being investigated as an anti-angiogenic and anti-neoplastic agent in patients diagnosed with esophageal carcinoma, hormone refractory prostate cancer, colorectal cancer, and breast cancer (clinical trials.gov identifier: NCT00176800, NCT00150995, NCT00176774, NCT00195091, respectively) (21). ATN-224 is a bis-choline salt that is a second generation analog of TM, with superior stability and a faster onset of action. ATN-224 has completed phase I studies in solid tumors and in hematological malignancies and is currently under investigation in several phase II trials as an anti-angiogenic and anti-neoplastic agent in a variety of cancers (NCT00383851 and NCT00405574, respectively).

We hypothesized that combination of copper chelation with oHSV would enhance its antitumor efficacy by both enhancing its serum stability and inhibiting angiogenesis. In this report, we showed that treatment of mice with ATN-224 can rescue serum mediated inhibition of viral replication, and enhance antitumor efficacy of oHSV, permitting its systemic delivery. To our knowledge, this is the first study to demonstrate the utility of combining ATN-224 and oHSV to allow systemic delivery, and enhance therapeutic efficacy.

Materials and methods

Cell lines, Reagents and Viruses

Gli36 EGFR, U87 EGFR, and U251T3 human glioma cells, Vero cells, and X12-V2 primary tumor derived cells were cultured in Dulbecco's modified Eagle's medium (DMEM; Gibco BRL) supplemented with 10% fetal bovine serum (Gibco BRL), 100 units of penicillin/ml, and 10mg of streptomycin/ml (22). All cell lines were maintained at 37 °C in a humidified atmosphere at 5% CO₂. To verify that ATN-224's effect on oHSV did not depend on a specific virus mutation, we have used three different viruses with different viral backbones in this study. The construction and generation of rHSVQ1, rQnestin34.5, and hrR3 virus have been previously described, and differences in their structure were summarized in Supplementary Table S1. (7, 23). All viruses were propagated in Vero cells, purified, and infectious virus titers (plaque forming unit per ml, pfu/ml) were determined by plaque forming unit assay on Vero cells (10, 24–25). Tetrathiomolybdate analog, ATN-224, was kindly provided by Dr. Andrew P. Mazar (Northwestern University, Evanston, IL). ATN-224, cupric chloride was filter sterilized and made fresh each time prior to use. For in vitro experiments, ascorbate buffer was used as a reducing agent as described (26).

Cell viability and viral replication assays

For cell viability assay, the indicated cells were infected with oHSV (MOI of 0.1) pre-incubated with ascorbate buffer ± copper (1 mg/L) ± ATN-224 (32 μM) for 30 min at RT. 48 hr post infection, the cells were fixed with 1% glutaraldehyde, and stained with 0.5% crystal violet. After washing, the crystals were dissolved in Sorenson's buffer (0.025 M sodium citrate, 0.025 mol/l citric acid in 50% ethanol) and plates were then read on a microplate reader at 590 nm. All assays were performed in triplicate. For replication assay, the indicated cells were harvested 48 hrs post oHSV infection, and the amount of infectious virus particles in cells and media was determined by performing a standard plaque forming unit assay on Vero cells, as previously described (10).

Animal Surgery

All mice experiments were housed and handled in accordance with the Subcommittee on Research Animal Care of the Ohio State University guidelines and have been approved by the Institutional Review Board. Female athymic nu/nu mice (Charles River Laboratories, Frederick, MD), 4–5-week-old for subcutaneous tumor model and 6–8 week-old for intracranial tumor model, were used for all studies. For subcutaneous tumor studies, glioma cells (U251T3, 1.5×10^7) were implanted subcutaneously into the rear flank of female athymic nude mice. When tumors reached an average size of 100 mm³, mice were randomized and treated with PBS or ATN-224 (0.7 mg/day dissolved in 100 ul PBS) by daily gavage (n=10). Thirteen days later PBS or rQnestin34.5 was administered intratumorally (1×10^5 pfu). Tumor volume was calculated using the following formula: volume = $0.5LW^2$ as described (27).

For intracranial tumor studies, anesthetized nude mice were fixed in a stereotactic apparatus, and a burr hole was drilled 2 mm lateral to the bregma. U87 EGFR cells (1×10^5) were

then implanted at a depth of 3 mm. 3 days post tumor implantation, mice were randomized to be fed with PBS or ATN-224 (0.7 mg/day dissolved in 100 μ l PBS) by daily gavage. Ten days following tumor cell implantation, the mice were anesthetized again and injected intratumorally with PBS or 5×10^4 pfu of rQnestin34.5 at the same location. Animals were observed daily and were euthanized at the indicated time points when they become moribund, lethargic, anorexic, dehydrated, or distressed.

For ex vivo serum rescue assays, female nude mice were fed with PBS/ATN-224 by daily gavage for ten days. Blood was collected from sub-mandibular vein and serum was harvested as described (28). 20 μ l of serum diluted with 20 μ l of Hank's buffered salt solution (HBSS) was incubated with rQnestin34.5 (2×10^3 pfu) for 1 hr at 37 °C and the amount of virus particles was measured by a standard plaque assay. For in vivo serum rescue assay, mice were fed with PBS/ATN-224 for seven days and then hrR3 (2×10^7 pfu) was administered by tail vein injection. 20 minutes post virus injection serum was harvested and the number of infectious virus particles present was determined.

PCR analysis

To measure viral gene copy in vivo, tumor bearing mice were sacrificed and total DNA from the tumors was purified (Master Pure™ Complete DNA & RNA Purification Kit, Epicentre Biotechnologies), as manufacturer's instruction. Viral gene copy present in the tumors was measured by determining the total number of copies of the HSV specific ICP4 gene using quantitative real-time PCR (qPCR) analysis. ICP4 primers used were: sense, 5'-CGACACGGATCCACGACCC-3' and anti-sense, 5'-ATCCCCCTCCCGCGCTTCGTCCG-3'. Total oHSV gene copy was determined by generating a linear regression curve using a plasmid containing the ICP4 of HSV-1 viral gene (Dr. Deborah Parris at The Ohio State University). To measure changes in angiogenic gene expression, subcutaneous glioma (U251T3) bearing mice were sacrificed and RNA was purified from the ipsilateral hemisphere using RNeasy lipid tissue (Qiagen, Cat. 75842). Changes in mouse and human angiogenic gene expression was measured using commercially available primers (murine VEGF, Cat# MP218181, human VEGF, Cat# HP202779, murine IL-8, Cat# MP206804, human IL-8, Cat# HP200599, Origene, Rockville, MD).

Antibodies

The following antibodies were used for immunohistochemistry: rat anti-mouse CD31 (PharMingen, San Jose, CA), polyclonal rabbit anti-herpes simplex virus type 1 (DAKO, Cambridge, UK), Peroxidase-conjugated donkey anti-rabbit (Jackson ImmunoResearch Laboratories, West Grove, PA) and biotin-conjugated goat anti-rat IgG (BD Biosciences PharMingen, San Diego, CA).

DCE-MRI imaging

Mice bearing intracranial tumors treated with rQnestin34.5 \pm ATN-224 (n=4) were imaged 3 days after oHSV treatment using T2-weighted RARE imaging sequence (TR=2500 ms, TE=12 ms, Rare Factor=8, navgs=4). The imaging was performed using a Bruker Biospin 94/30 magnet (Bruker Biospin, Karlsruhe Germany) as previously described (10). The mean C(t), IAUC, and CIAUC curves were evaluated and compared for the rQnestin34.5, and rQnestin34.5+ATN-224-treated mice at day 13 from tumor implantation. The rate constant, K_{trans} , and the extravascular extracellular space, v_e , were determined by nonlinear curve fitting the Gd concentration, C(t), over a 20 minute time period post Gd injection. Color-coded maps for K_{trans} and v_e were created to visualize the spatial distribution of Gd in the tumor. Histograms of K_{trans} and v_e for the entire tumors were calculated and median values were compared between the treatment groups.

Statistical Analysis

Student's *t*-test was used to analyze changes in cell killing, viral replication, microvessel density, and gene copy changes. Two-tailed *P*-values are displayed. A *P* value <0.05 was considered statistically significant. All error bars displayed are shown as standard deviations, and all graphs were generated using Microsoft Excel. To analyze mice survival data, Kaplan–Meier curves were compared using the log rank test and Breslow (Generalized Wilcoxon) tests. All statistical analyses were performed with the use of SPSS statistical software (version 14.0; SPSS, Chicago, IL).

Results

Impact of ATN-224 treatment on oHSV therapeutic efficacy in subcutaneous and intracranial glioma

We have previously shown that treatment with anti-angiogenic agents increases virus propagation in tumors (7). Here we examined the therapeutic efficacy of combining ATN-224 with oHSV in two different human glioma xenograft models. Mice bearing subcutaneous U251T3 tumors (100 mm³ in volume) were randomized and systemically administered ATN-224 (0.7mg/day) or PBS via daily gavage (n=10), and were then treated intra-tumorally with either oHSV (rQnestin34.5) or PBS. PBS treated mice showed rapid tumor growth, while mice treated with rQnestin34.5 or ATN-224 alone showed a significant reduction of tumor growth (Fig. 1A). When mice were treated with both ATN-224 and rQnestin34.5, there was an even greater reduction in tumor growth with seven out of ten mice showing a complete response compared to only 1 out of ten mice when treated with either agent alone. On day 25, the mean tumor volumes in mice treated with ATN-224 alone, rQnestin34.5 alone, and ATN-224 plus rQnestin34.5 were 250.1 ± 106.7 , 153.9 ± 50 , and 21.5 ± 15.3 , respectively. These data correlate to 49.7, 69, and 95.7% tumor growth inhibition as compared to PBS control (Fig. 1A).

The enhanced anti-tumor efficacy of oHSV combined with ATN-224 was also observed in mice bearing intracranial glioma (Fig. 1B). Mice bearing orthotropic U87 EGFR human glioma were treated with ATN-224 or PBS for seven days prior to being treated with a single dose of rQnestin34.5 (5×10^4 pfu) or PBS by direct intra-tumoral injection. The survival of mice in each group (n=8/group) was analyzed by Kaplan-Meier curves. These results showed a significant improvement in median survival of mice treated with ATN-224 plus rQnestin34.5 over that of single agent alone (median survivals: 19, 25 and 40 days for mice treated with ATN-224, rQnestin34.5, and ATN-224 + rQnestin34.5 respectively).

Combination of ATN-224 and oHSV decreases blood vessel formation and vascular hyper-permeability in tumors

To evaluate the impact of ATN-224 on glioma angiogenesis, we evaluated tumor microvessel density in subcutaneous and intracranial tumors. Fig. 2A shows photomicrographs of U251T3 subcutaneous tumor sections immunostained for CD31 to highlight endothelial cells. Quantification of CD31 staining showed a statistically significant reduction in microvessel density in tumors treated with ATN-224 (Fig. 2B). More importantly, a significant inhibition in vessel density was also observed in tumors derived from mice treated with both ATN-224 and rQnestin34.5 compared to mice treated with rQnestin34.5 alone. ATN-224 has been previously shown to reduce the expression of angiogenic cytokines (29). To evaluate if ATN-224 reduced the expression of tumoral and host angiogenic cytokines in glioma bearing mice, we measured changes in both mouse and human angiogenic factors, VEGF and IL-8. Fig. 2C shows a significant down regulation of both tumoral and host VEGF and IL-8 factors when mice are treated with ATN-224 in addition to rQnestin34.5, as compared to mice treated with rQnestin34.5 alone.

To evaluate the physiological consequence of ATN-224 on perfusion in oHSV-treated brain tumors, we performed dynamic contrast enhanced magnetic resonance imaging (DCE-MRI) of intracranial glioma-bearing mice. Fig. 3A shows representative images of coronal brain sections of mice treated with rQnestin34.5 or ATN-224 plus rQnestin34.5. The top panel shows contrast enhancement of tumor-bearing mice imaged 3 days after the oHSV treatment and immediately following administration of gadolinium diethylene-triamine penta-acetic acid (Gd-DTPA). Contrast enhancement at the site of oHSV injection was evident in all of the oHSV-treated mice. The middle and bottom panels are parametric images showing changes in K_{trans} (blood-to-tissue transfer constant or vessel leakiness) and v_e (volume of contrast in the extravascular and extracellular space per unit volume of tissue) between PBS- and ATN-224-fed animals treated with rQnestin34.5 respectively. Quantification of the parameters revealed a significant reduction in both K_{trans} (60.4%, $P=0.0399$) and v_e (56.3%, $P=0.0316$) in ATN-224 plus rQnestin34.5-treated animals compared to rQnestin34.5 alone-treated animals (Fig. 3A–B). Interestingly in mice that were not treated with rQnestin34.5, ATN-224 did not alter K_{trans} or v_e (Supplementary Fig. S1). The reduction in vascular perfusion and leakiness indicated by MRI analysis was further investigated histologically. Fig. 3C are representative H&E- and CD31-stained images of tumor bearing brain sections, showing increased necrosis (asterix) and reduced vessel formation in mice treated with ATN-224 in addition to rQnestin34.5 compared to mice treated with rQnestin34.5 alone. Quantification of CD31 staining revealed the reduced vessel formation to be statistically significant (Fig. 3D).

ATN-224 increases oHSV propagation in tumors

Interestingly, even though ATN-224 was found to be antiangiogenic in intracranial U87 EGFR tumors, ATN-224 treatment alone did not increase survival of these mice (Fig. 1B). To evaluate if increased efficacy was also due to increased oHSV propagation *in vivo*, we compared viral distribution of rQnestin34.5 in mice fed with PBS to mice fed with ATN-224. Fig. 4A shows representative microphotographs of HSV-1 immuno-stained brain sections of U87 EGFR intracranial tumor bearing mice. While tumors from mice treated with rQnestin34.5 showed some staining for virus in tumors, the entire tumor section was highly positive for HSV-1 staining in tumors when mice were fed ATN-224 (Fig. 4A). Similarly, HSV-1 staining of U251T3 subcutaneous tumors showed enhanced virus propagation when mice were fed ATN-224 compared to mice fed PBS (Fig. 4B). No staining was observed in tumors injected with PBS instead of oHSV (Supplementary Fig. S2). Consistent with increased HSV-1 staining, we found that the total viral yield in tumors of animals treated with ATN-224 plus rQnestin34.5 was about 3.31-fold higher than in mice treated with rQnestin34.5 alone ($P=0.018$) (Fig. 4C).

ATN-224 rescues copper-mediated inhibition of oHSV replication and cytotoxicity *in vitro* and *in vivo*

Apart from increasing angiogenesis, copper (Copper) has been shown to inhibit wild-type HSV-1 replication in cultured cells *in vitro* (16). Thus, we tested if ATN-224's ability to chelate copper directly increases oHSV propagation. We first tested the effect of Copper on the ability of oHSV to replicate *in vitro*. Stable glioma cell lines, U251T3 and GLI36 EGFR, and a patient-derived glioma cell, X12-V2, were infected with rQnestin34.5 or rHSVQ1 at an MOI of $0.1 \pm$ Copper. Uninfected cells were used as negative control. As both viruses encode for GFP, fluorescent microscopy was utilized to visualize oHSV-infected cells. A significant reduction in GFP positive cells was apparent when cells were infected in the presence of copper (Fig. 5A, and Supplementary Fig. S3A).

Along with reduced infection, both rQnestin 34.5 and rHSVQ1 demonstrated significantly reduced glioma cell killing when the viruses were pre-incubated with copper (Fig. 5B, and

Supplementary Fig. S3B). Next, we investigated the ability of ATN-224 to rescue copper-mediated inhibition of oHSV by fluorescent microscopy and by measuring viral replication and cytolysis (Fig. 5 C–E). Fluorescent microscopy of GFP positive cells showed that ATN-224 treatment could rescue Copper-mediated inhibition of glioma cell infection (Fig. 5C). More significantly, ATN-224 treatment completely reversed the Copper-mediated inhibition of oHSV replication and oncolysis (Fig. 5D–E). ATN-224 treatment in the absence of Copper has no significant effect on the proliferation of glioma cells *in vitro* or the ability of rQnestin34.5 to kill glioma cells (Supplementary Fig. S4).

To examine the physiological relevance of these results, we investigated the effect of ATN-224 on oHSV replication in *ex vivo* and *in vivo* models. Serum from mice fed ATN-224 or PBS was incubated with rQnestin34.5 for 30 minutes and the ability of the virus to form plaques on vero cells was measured by a standard plaque assay. Fig. 6A, and Supplementary Fig. S5 shows an increase in GFP positive infected cells treated with virus incubated with serum obtained from ATN-224 treated mice compared to control mice. Consistent with this, quantification of oHSV showed a significant increase in survived infectious virus particles in samples treated with serum obtained from ATN-224 fed mice compared to control mice (Fig. 6B). To examine if the serum stability of oHSV was increased *in vivo*, mice fed with ATN-224 or PBS were injected with a single dose of oHSV (hrR3; 2×10^7) via tail vein. Twenty minutes post viral injection, mouse serum was harvested to evaluate the amount of infectious virus particles. Fig. 6C shows a significant increase in the number of virus particles present in serum from ATN-224 treated mice compared to that from PBS-treated control mice ($P < 0.01$). Collectively these results suggested that ATN-224 treatment increased the serum stability of oHSV *in vivo*.

ATN-224 treatment increases systemic delivery of oHSV

Next we tested if treatment with ATN-224 could be utilized to improve systemic delivery of oHSV to tumors. U251T3 subcutaneous tumor-bearing mice were treated with PBS or ATN-224 and oHSV (hrR3 at 1×10^7 pfu) was injected intravenously via tail vein on day 7 post-commencement of ATN-224 or PBS treatment. Three days post oHSV treatment, tumors were harvested and total DNA was analyzed for viral gene copy. Fig. 6D shows a 2.21 fold increase in the number of oHSV particles detected in the tumor tissues from mice treated with ATN-224 compared to mice treated with PBS. Immunostained sections derived from these tumors for HSV-1 shows increased oHSV propagation when mice were fed ATN-224 compared to PBS (Fig. 6E).

As ATN-224 treatment increased virus stability in blood and increased virus presence in tumor tissue after systemic delivery, we assessed the effect of ATN-224 on the antitumor efficacy of intravenous oHSV administration. Mice bearing subcutaneous U251T3 tumors (150 mm^3) were fed ATN-224 or PBS and then injected intravenously with oHSV (rQnestin34.5 at 1×10^7), and tumor growth was monitored. Fig. 6F shows an enhancement of the antitumor efficacy of oHSV in mice fed with ATN-224. Importantly, five out of eight mice treated with ATN-224 and rQnestin34.5 in combination achieved complete regression. These results suggest that ATN-224 can improve the efficacy of oHSV and also enhance its systemic delivery.

Discussion

Oncolytic virus (OV) therapy, including oncolytic herpes simplex virus (oHSV), is a promising biological approach for the treatment of malignant tumors, and OVs are currently under evaluation for their safety and efficacy in human patients (1, 30). While recent Phase I/II trials have shown acceptable safety profiles in patients, several barriers within the host limit OV efficacy (3, 31). Thus, efforts to develop innovative strategies to enhance the

therapeutic efficacy of these agents are in high demand. Here we tested the effect of ATN-224, an anti-angiogenic and novel copper chelator, on oHSV therapy. Our results demonstrate that combining ATN-224 with oHSV for the treatment of glioma remarkably enhances its antitumor efficacy compared to oHSV treatment alone due to both the inhibition of angiogenesis and the direct rescue of copper-mediated inhibition of oHSV.

Copper has been shown to increase endothelial cell proliferation in vitro and increase angiogenesis in vivo (12, 32). The angiogenic effects of copper have been attributed to an increased stabilization of HIF1 and an increased production and secretion of several angiogenic factors including FGF, IL-8, and VEGF (32–35). Additionally, increased levels of copper have been found accumulated within the malignant tissues of metastatic carcinoma and malignant glioma (36). Based on these results, copper depletion has been tested as an antiangiogenic strategy in preclinical animals and patients. Specifically, it has been shown that animals fed with a copper depleted diet have a significant reduction in serum copper levels, decreased copper staining of tumor cell nuclei, reduction in microvascular density, reduction in tumor volume, and reduction in endothelial cell turnover. Since reduction of brain tumor copper was observed even in CDPT rabbits, we believe it may not be necessary for ATN-224 to cross the BBB to reduce brain tumor copper levels. Interestingly, however, despite reduced tumor burden and angiogenesis, these animals also showed an increase in vascular permeability (breakdown of the blood-brain barrier) as well as peri-tumoral brain edema and thus showed no significant improvement in survival (37). Consistent with these results, reduction in serum copper levels achieved by diet did not correlate with increased survival in patients diagnosed with glioblastoma multiforme (38).

ATN-224, bis (2-hydroxyethyl) trimethylammonium, is a second generation analog of ammonium terathiomolybdate (TM) that is FDA approved for Wilson's disease. Apart from copper chelation, ATN-224 has been shown to have copper independent antiangiogenic effects (39–40), to directly inhibit tumor cell invasion, and to induce cancer cell anoikis (19). Based on promising preclinical data, it is currently being investigated as an anticancer agent in several clinical trials (NCT00383851, NCT00405574) (41). Here we show that ATN-224 treatment in combination with oHSV significantly improves antitumor efficacy of oHSV. Consistent with previous studies on animals fed with a copper depleted diet, we found ATN-224 treatment of tumor bearing mice reduced tumoral angiogenesis and slowed down tumor growth of animals bearing subcutaneous tumors.

As noted above, while copper depletion has been shown to reduce vessel density, it has also been shown to increase vascular edema in tumor bearing animals (37). To investigate this issue in our model, we used DCE-MRI to assess changes in K_{trans} and v_e in mice treated with ATN-224 compared to mice treated with PBS in the absence of oHSV treatment. We found no change in either dimension indicating that in our model ATN-224 treatment did not increase tumoral vascular leakage (data not shown). Interestingly, in the context of oHSV-treated tumors, ATN-224 treatment reduced both K_{trans} and v_e , suggesting a reduced vascular leakage in oHSV-treated tumors. It will be interesting to investigate how ATN-224's copper-independent anti-angiogenic and anti-tumorigenic effects may account for these differences.

Copper has also been shown to be a potent inhibitor of several enveloped and non-enveloped DNA and RNA viruses (42), possibly due to the inhibition of viral DNA replication and copper mediated DNA damage (17, 26). Based on these observations, topical formulations containing copper are currently being evaluated as antiviral agents in patients with herpetic skin lesions (15). Here we show for the first time that serum mediated inhibition of oHSV, can be reduced by copper chelating agent ATN-224 resulting in improved oHSV's serum

stability and therapeutic efficacy. Clinically, oHSV has been given by direct intra-tumoral injections. These findings may facilitate its systemic delivery and provide a significant framework for clinical translation.

Supplementary Material

Refer to Web version on PubMed Central for supplementary material.

Acknowledgments

We would like to thank Dr Quintin Pan for helpful suggestions and advice for the use of ATN-224 in animals.

Grant Support

This work was supported by funding from the National Institutes of Health grant (1R01NS064607, and 1R01CA150153 to B.K.; 5R01CA119298-5 to JCG.).

References

1. Wollmann G, Ozduman K, van den Pol AN. Oncolytic virus therapy for glioblastoma multiforme: concepts and candidates. *Cancer J.* 2012; 18:69–81. [PubMed: 22290260]
2. Cassidy KA, Parker JN. Herpesvirus vectors for therapy of brain tumors. *Open Virol J.* 2010; 4:103–108. [PubMed: 20811578]
3. Kaur B, Chiocca EA, Cripe TP. Oncolytic HSV-1 Virotherapy: Clinical Experience and Opportunities for Progress. *Curr Pharm Biotechnol.* 2011
4. Kurozumi K, Hardcastle J, Thakur R, Shroll J, Nowicki M, Otsuki A, et al. Oncolytic HSV-1 infection of tumors induces angiogenesis and upregulates CYR61. *Mol Ther.* 2008; 16:1382–1391. [PubMed: 18545226]
5. Aghi M, Rabkin SD, Martuza RL. Angiogenic response caused by oncolytic herpes simplex virus-induced reduced thrombospondin expression can be prevented by specific viral mutations or by administering a thrombospondin-derived peptide. *Cancer Res.* 2007; 67:440–444. [PubMed: 17234749]
6. Libertini S, Iacuzzo I, Perruolo G, Scala S, Ierano C, Franco R, et al. Bevacizumab increases viral distribution in human anaplastic thyroid carcinoma xenografts and enhances the effects of E1A-defective adenovirus dl922-947. *Clin Cancer Res.* 2008; 14:6505–6514. [PubMed: 18927290]
7. Kurozumi K, Hardcastle J, Thakur R, Yang M, Christoforidis G, Fulci G, et al. Effect of tumor microenvironment modulation on the efficacy of oncolytic virus therapy. *J Natl Cancer Inst.* 2007; 99:1768–1781. [PubMed: 18042934]
8. Liu TC, Castelo-Branco P, Rabkin SD, Martuza RL. Trichostatin A and oncolytic HSV combination therapy shows enhanced antitumoral and antiangiogenic effects. *Mol Ther.* 2008; 16:1041–1047. [PubMed: 18388912]
9. Hardcastle J, Kurozumi K, Dmitrieva N, Sayers MP, Ahmad S, Waterman P, et al. Enhanced antitumor efficacy of vasculostatin (Vstat120) expressing oncolytic HSV-1. *Mol Ther.* 2010; 18:285–294. [PubMed: 19844198]
10. Yoo JY, Haseley A, Bratasz A, Chiocca EA, Zhang J, Powell K, et al. Antitumor Efficacy of 34.5ENVE: A Transcriptionally Retargeted and "Vstat120"-expressing Oncolytic Virus. *Mol Ther.* 2012; 20:287–297. [PubMed: 22031239]
11. Israyelyan A, Shannon EJ, Baghian A, Kearney MT, Kousoulas KG. Thalidomide suppressed the growth of 4T1 cells into solid tumors in Balb/c mice in a combination therapy with the oncolytic fusogenic HSV-1 OncdSyn. *Cancer Chemother Pharmacol.* 2009; 64:1201–1210. [PubMed: 19308409]
12. Hu GF. Copper stimulates proliferation of human endothelial cells under culture. *J Cell Biochem.* 1998; 69:326–335. [PubMed: 9581871]

13. Soncin F, Guitton JD, Cartwright T, Badet J. Interaction of human angiogenin with copper modulates angiogenin binding to endothelial cells. *Biochem Biophys Res Commun.* 1997; 236:604–610. [PubMed: 9245697]
14. Turecky L, Kalina P, Uhlikova E, Namerova S, Krizko J. Serum ceruloplasmin and copper levels in patients with primary brain tumors. *Klin Wochenschr.* 1984; 62:187–189. [PubMed: 6323815]
15. Clewell A, Barnes M, Endres JR, Ahmed M, Ghambeer DK. Efficacy and Tolerability Assessment of a Topical Formulation Containing Copper Sulfate and *Hypericum perforatum* on Patients With Herpes Skin Lesions: A Comparative, Randomized Controlled Trial. *J Drugs Dermatol.* 2012; 11:209–215. [PubMed: 22270204]
16. Panteva M, Varadinova T, Turel I. Effect of Copper Acyclovir Complexes on Herpes Simplex Virus Type 1 and Type 2 (HSV-1, HSV-2) Infection in Cultured Cells. *Met Based Drugs.* 1998; 5:19–23. [PubMed: 18475820]
17. Shishkov S, Varadinova T, Panteva M, Bontchev P. Effect of Complexes of Zinc, Cobalt and Copper With D-Aminosugars on the Replication of Herpes Simplex Virus Type 1 (HSV-1). *Met Based Drugs.* 1997; 4:35–38. [PubMed: 18475763]
18. Pan Q, Kleer CG, van Golen KL, Irani J, Bottema KM, Bias C, et al. Copper deficiency induced by tetrathiomolybdate suppresses tumor growth and angiogenesis. *Cancer Res.* 2002; 62:4854–4859. [PubMed: 12208730]
19. Kumar P, Yadav A, Patel SN, Islam M, Pan Q, Merajver SD, et al. Tetrathiomolybdate inhibits head and neck cancer metastasis by decreasing tumor cell motility, invasiveness and by promoting tumor cell anoikis. *Mol Cancer.* 2010; 9:206. [PubMed: 20682068]
20. Pan Q, Rosenthal DT, Bao L, Kleer CG, Merajver SD. Antiangiogenic tetrathiomolybdate protects against Her2/neu-induced breast carcinoma by hypoplastic remodeling of the mammary gland. *Clin Cancer Res.* 2009; 15:7441–7446. [PubMed: 19934283]
21. Lin J, Zahurak M, Beer TM, Ryan CJ, Wilding G, Mathew P, et al. A non-comparative randomized phase II study of 2 doses of ATN-224, a copper/zinc superoxide dismutase inhibitor, in patients with biochemically recurrent hormone-naive prostate cancer. *Urol Oncol.* 2011
22. Dmitrieva N, Yu L, Viapiano M, Cripe TP, Chiocca EA, Glorioso JC, et al. Chondroitinase ABC I-mediated enhancement of oncolytic virus spread and anti tumor efficacy. *Clin Cancer Res.* 2010
23. Kambara H, Okano H, Chiocca EA, Saeki Y. An oncolytic HSV-1 mutant expressing ICP34.5 under control of a nestin promoter increases survival of animals even when symptomatic from a brain tumor. *Cancer Res.* 2005; 65:2832–2839. [PubMed: 15805284]
24. Terada K, Wakimoto H, Tyminski E, Chiocca EA, Saeki Y. Development of a rapid method to generate multiple oncolytic HSV vectors and their in vivo evaluation using syngeneic mouse tumor models. *Gene Ther.* 2006; 13:705–714. [PubMed: 16421599]
25. Sundaresan P, Hunter WD, Martuza RL, Rabkin SD. Attenuated, replication-competent herpes simplex virus type 1 mutant G207: safety evaluation in mice. *J Virol.* 2000; 74:3832–3841. [PubMed: 10729157]
26. Sagripanti JL, Routson LB, Bonifacino AC, Lytle CD. Mechanism of copper-mediated inactivation of herpes simplex virus. *Antimicrob Agents Chemother.* 1997; 41:812–817. [PubMed: 9087495]
27. Haseley A, Boone S, Wojton J, Yu L, Yoo JY, Yu J, et al. Extracellular matrix protein CCN1 limits oncolytic efficacy in glioma. *Cancer Res.* 2012
28. Wakimoto H, Ikeda K, Abe T, Ichikawa T, Hochberg FH, Ezekowitz RA, et al. The complement response against an oncolytic virus is species-specific in its activation pathways. *Mol Ther.* 2002; 5:275–282. [PubMed: 11863417]
29. Hassouneh B, Islam M, Nagel T, Pan Q, Merajver SD, Teknos TN. Tetrathiomolybdate promotes tumor necrosis and prevents distant metastases by suppressing angiogenesis in head and neck cancer. *Mol Cancer Ther.* 2007; 6:1039–1045. [PubMed: 17363496]
30. Schmidt C. Amgen spikes interest in live virus vaccines for hard-to-treat cancers. *Nat Biotechnol.* 2011; 29:295–296. [PubMed: 21478830]
31. Smith E, Breznik J, Lichty BD. Strategies to enhance viral penetration of solid tumors. *Hum Gene Ther.* 2011; 22:1053–1060. [PubMed: 21443415]

32. Sen CK, Khanna S, Venojarvi M, Trikha P, Ellison EC, Hunt TK, et al. Copper-induced vascular endothelial growth factor expression and wound healing. *Am J Physiol Heart Circ Physiol.* 2002; 282:H1821–H1827. [PubMed: 11959648]
33. Rajalingam D, Kumar TK, Yu C. The C2A domain of synaptotagmin exhibits a high binding affinity for copper: implications in the formation of the multiprotein FGF release complex. *Biochemistry.* 2005; 44:14431–14442. [PubMed: 16262243]
34. Martin F, Linden T, Katschinski DM, Oehme F, Flamme I, Mukhopadhyay CK, et al. Copper-dependent activation of hypoxia-inducible factor (HIF)-1: implications for ceruloplasmin regulation. *Blood.* 2005; 105:4613–4619. [PubMed: 15741220]
35. Bar-Or D, Thomas GW, Yukl RL, Rael LT, Shimonkevitz RP, Curtis CG, et al. Copper stimulates the synthesis and release of interleukin-8 in human endothelial cells: a possible early role in systemic inflammatory responses. *Shock.* 2003; 20:154–158. [PubMed: 12865660]
36. Yoshida D, Ikeda Y, Nakazawa S. Quantitative analysis of copper, zinc and copper/zinc ratio in selected human brain tumors. *J Neurooncol.* 1993; 16:109–115. [PubMed: 8289088]
37. Brem SS, Zagzag D, Tsanaclis AM, Gately S, Elkouby MP, Brien SE. Inhibition of angiogenesis and tumor growth in the brain. Suppression of endothelial cell turnover by penicillamine and the depletion of copper, an angiogenic cofactor. *Am J Pathol.* 1990; 137:1121–1142. [PubMed: 1700617]
38. Brem S, Grossman SA, Carson KA, New P, Phuphanich S, Alavi JB, et al. Phase 2 trial of copper depletion and penicillamine as antiangiogenesis therapy of glioblastoma. *Neuro Oncol.* 2005; 7:246–253. [PubMed: 16053699]
39. Lowndes SA, Sheldon HV, Cai S, Taylor JM, Harris AL. Copper chelator ATN-224 inhibits endothelial function by multiple mechanisms. *Microvasc Res.* 2009; 77:314–326. [PubMed: 19323979]
40. Juarez JC, Betancourt O Jr, Pirie-Shepherd SR, Guan X, Price ML, Shaw DE, et al. Copper binding by tetrathiomolybdate attenuates angiogenesis and tumor cell proliferation through the inhibition of superoxide dismutase 1. *Clin Cancer Res.* 2006; 12:4974–4982. [PubMed: 16914587]
41. Lowndes SA, Adams A, Timms A, Fisher N, Smythe J, Watt SM, et al. Phase I study of copper-binding agent ATN-224 in patients with advanced solid tumors. *Clin Cancer Res.* 2008; 14:7526–7534. [PubMed: 19010871]
42. Sagripanti JL, Routson LB, Lytle CD. Virus inactivation by copper or iron ions alone and in the presence of peroxide. *Appl Environ Microbiol.* 1993; 59:4374–4376. [PubMed: 8285724]

Translational Relevance

Herpes simplex virus-1 derived oncolytic viruses (oHSV) represent a promising biological therapy that is currently being evaluated in cancer patients for safety and efficacy. A better understanding of the barriers faced by oHSVs can lead to the design of rational drug combinations which synergize with oncolytic viral therapy to improve patient outcome. Serum copper can support tumoral angiogenesis and can also inhibit wild type HSV-1 infection. ATN-224 is a second generation copper chelator that is currently being evaluated as an anti-neoplastic agent in patients. Here we show for the first time that ATN-224 enhances therapeutic efficacy of oHSV by increasing its serum stability and also permitting systemic delivery. Physiological concentration of copper directly inhibited oHSV replication and copper chelation by ATN-224 rescued the inhibitory effect of copper in vitro, ex vivo and in vivo. Our observation is a novel finding with global implications for enhancing the clinical efficacy of oHSV when delivered systemically in patients.

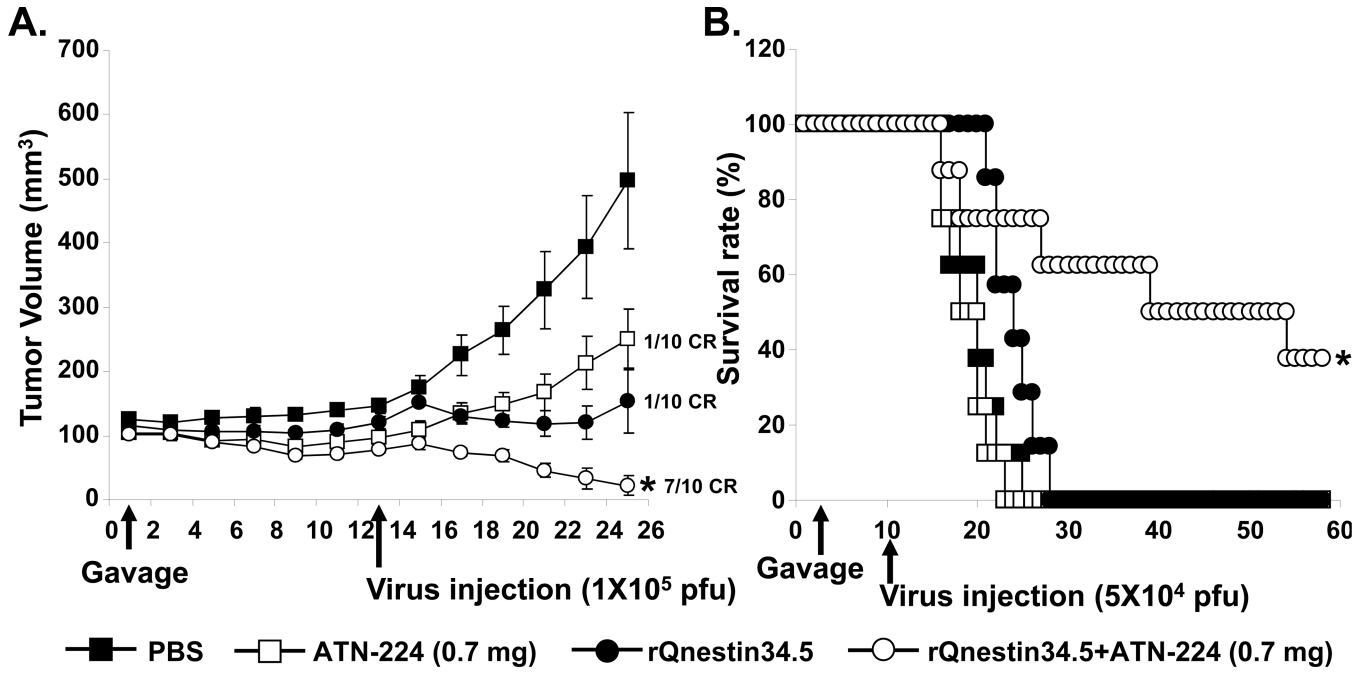


Figure 1. Impact of ATN-224 on anti-tumor efficacy of oHSV *in vivo*
 A) Tumor growth in subcutaneous (U251T3) tumor bearing mice treated with oHSV and ATN-224 or PBS (daily gavage). Thirteen days post initiation of gavage, mice were treated with rQnestin34.5 (1×10^5 pfu) or PBS by intra-tumoral injection ($n=10$). Data shown are the mean tumor volumes \pm SEM, at the indicated time points. *: $P < 0.05$ versus rQnestin34.5 alone. B) Kaplan-Meier survival curve of mice with intracranial tumors (U87 EGFR) treated with PBS or ATN-224 (daily gavage), and treated with PBS or rQnestin34.5. *: $P < 0.05$ compared to mice treated with only rQnestin34.5. The arrows indicate the time of treatment with oHSV and the start of ATN-224 treatment.

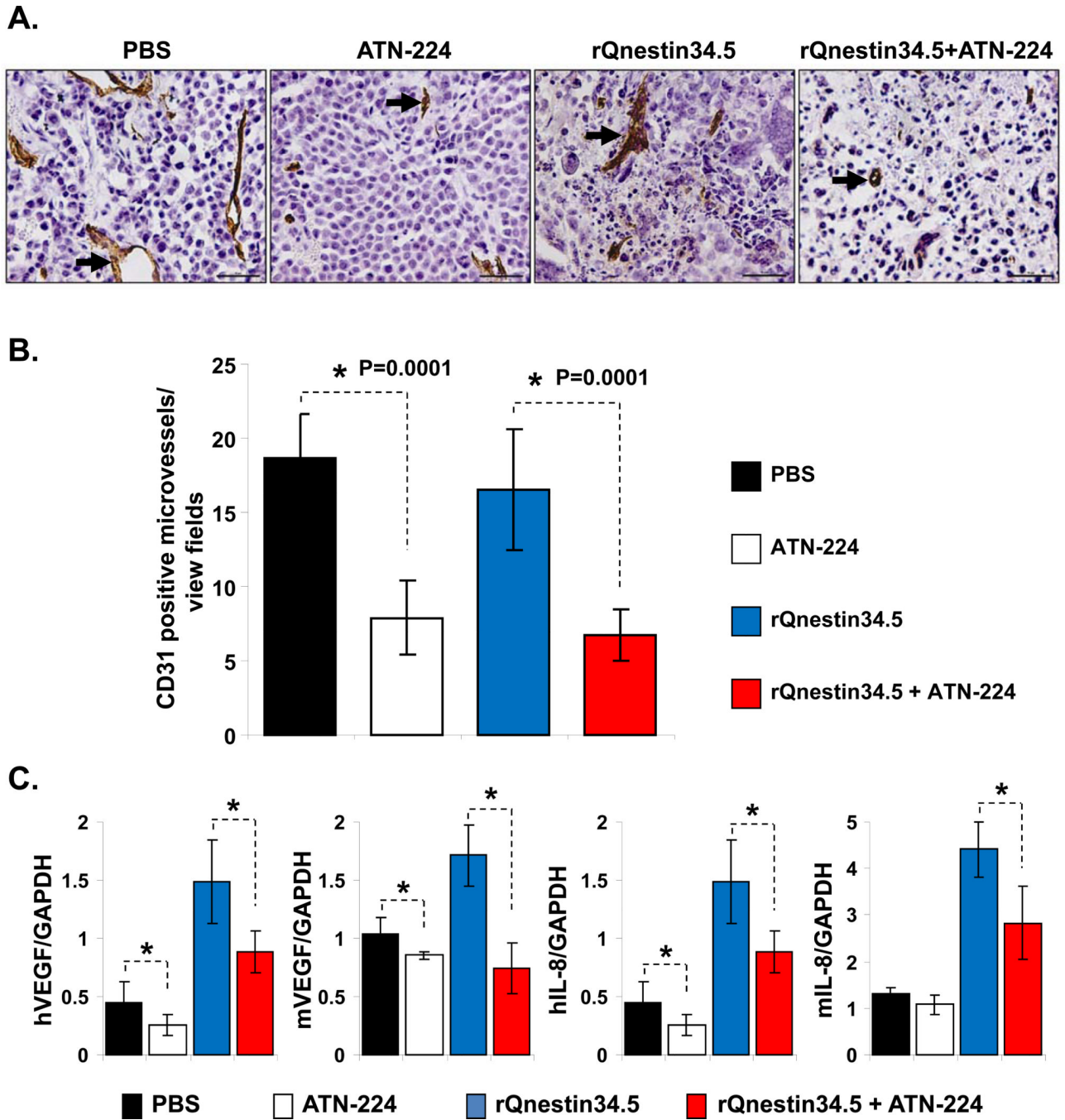


Figure 2. Antiangiogenic effect of ATN-224 on untreated and oHSV treated tumors

A) Representative (objective: 40×) photomicrographs of tumor sections stained with anti-CD31 antibody highlighting immunopositive endothelial cells (arrow heads). B) Quantification of mean microvessel density of tumors shown in A. *: $P < 0.05$ compared to PBS or rQnestin34.5 treated tumors. C) Impact of ATN-224 on tumoral and host cell derived VEGF and IL-8. Real time PCR analysis for changes in gene expression of angiogenic genes in tumor bearing hemispheres of mice three days after oHSV treatment. Data presented are fold changes in gene expression \pm SD relative to GAPDH. *: $P < 0.05$ compared to PBS or rQnestin34.5 treated tumors.

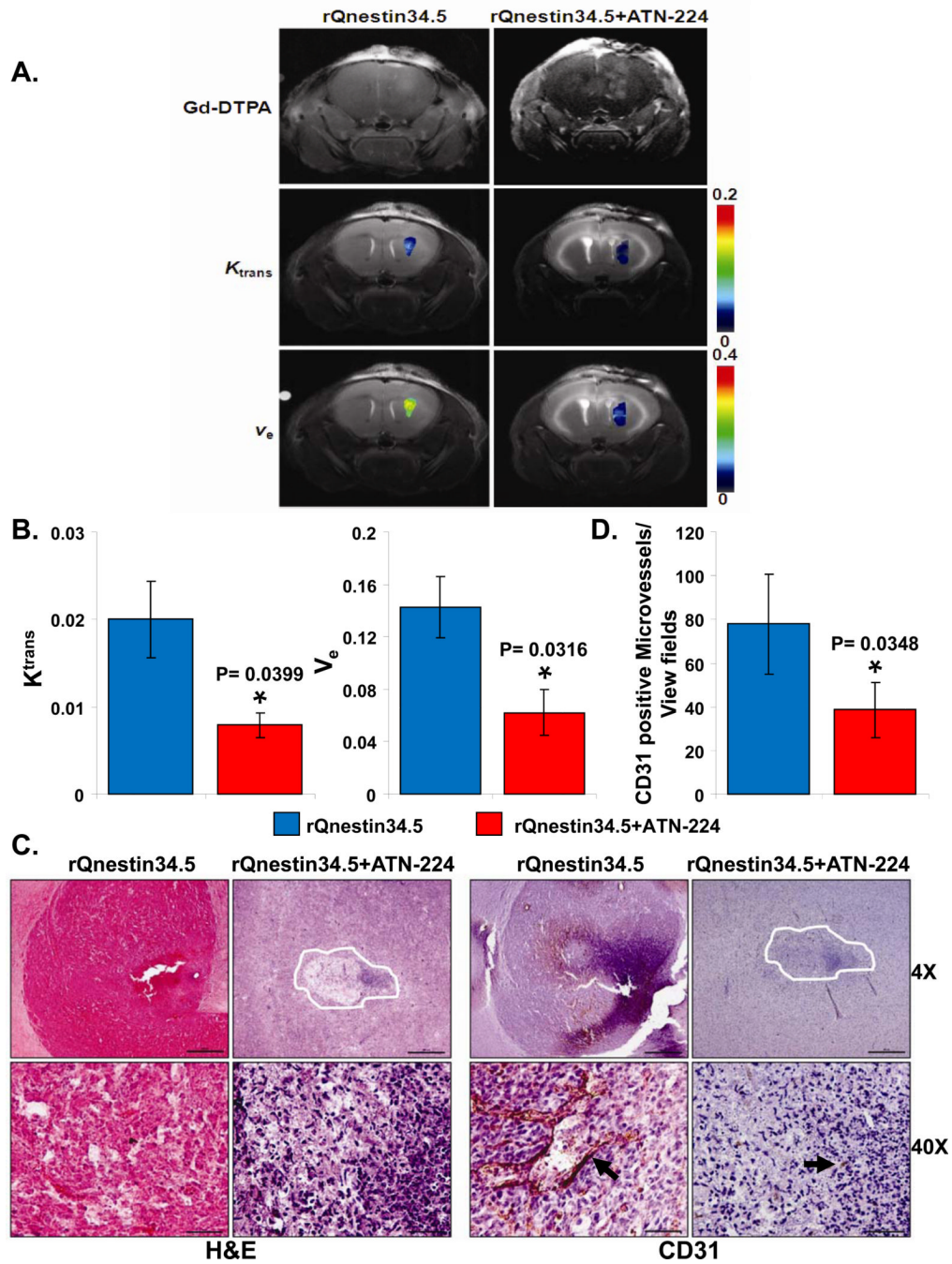


Figure 3. Changes in vascular perfusion in oHSV treated mice ± ATN-224

A) Contrast enhanced and color coded parametric images of coronal sections of mice three days after treatment with rQnestin34.5 ± ATN-224. Top panel shows Gd enhanced image (taken immediately after Gd injection) of one representative mouse/group imaged three days post treatment with rQnestin34.5. Middle panel shows color coded parametric images of K_{trans} in mice treated with rQnestin34.5 or rQnestin34.5 + ATN-224. Bottom panel shows color coded parametric images of v_e in mice treated with rQnestin34.5 or rQnestin34.5 + ATN-224. A shift towards red indicates a higher value. B) Quantification of changes in K_{trans} and v_e in oHSV treated tumors. Data shown are mean ± SD of four different mice. C) Representative photomicrographs of tumor sections stained with Hematoxylin and Eosin

(H&E) and anti-CD31 antibody highlighting endothelial cells. D) Quantification of mean microvessel density of tumors shown in C. *: $P < 0.05$ compared to rQnestin34.5 treated tumors.

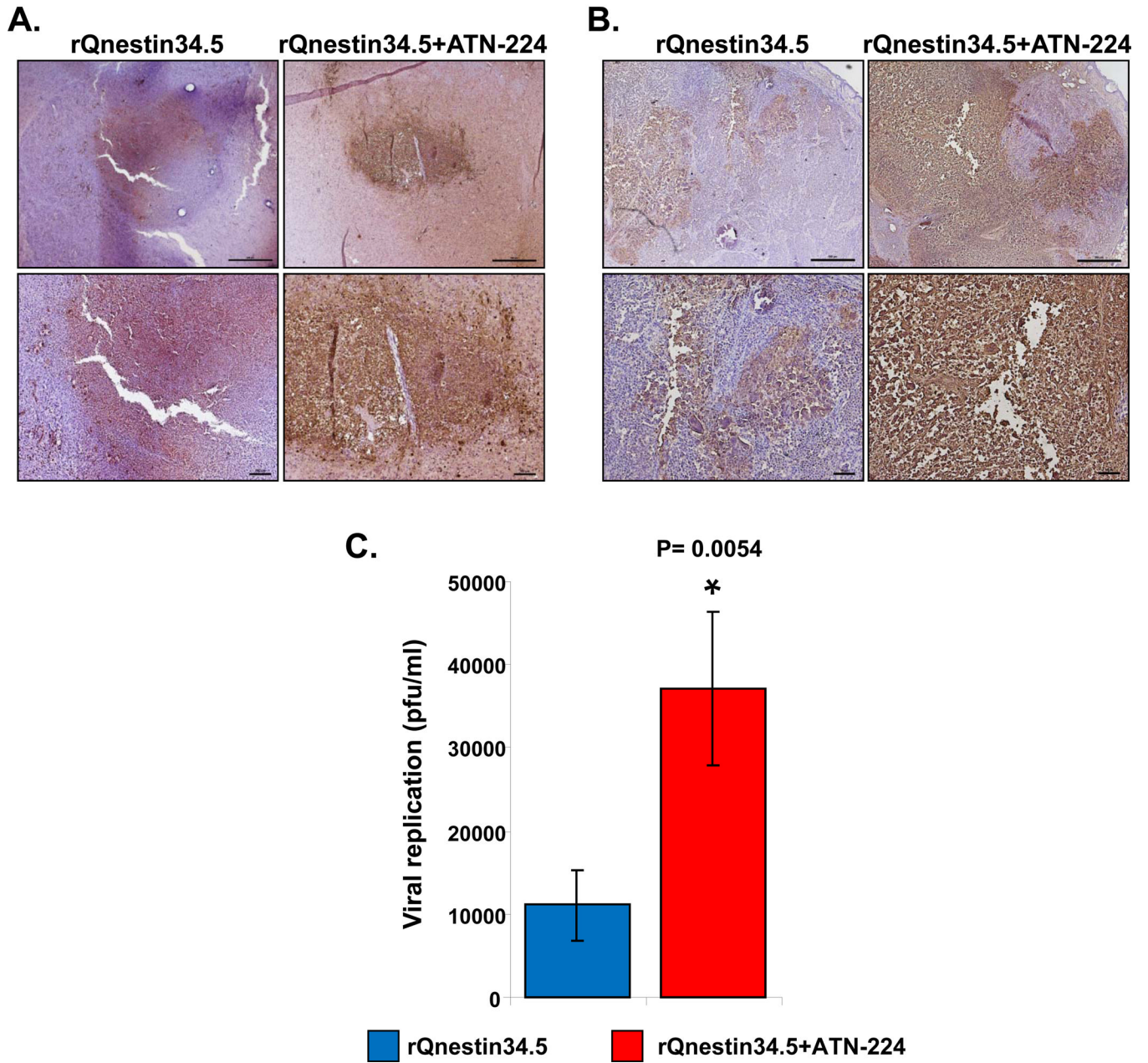


Figure 4. Impact of ATN-224 on oHSV propagation in vivo

A–B): Representative photomicrographs of tumor sections stained with anti-HSV-1 antibody highlighting virus propagation in mice bearing U87 EGFR intracranial tumors (A) and U251T3 subcutaneous tumors (B). C) Subcutaneous tumors treated with rQnestin34.5 from mice fed PBS or ATN-224 (as described in methods) were harvested three days after oHSV treatment and the total number of infectious virus was measured by a standard plaque assay (n=6). Data shown are mean pfu/ml ± SE.

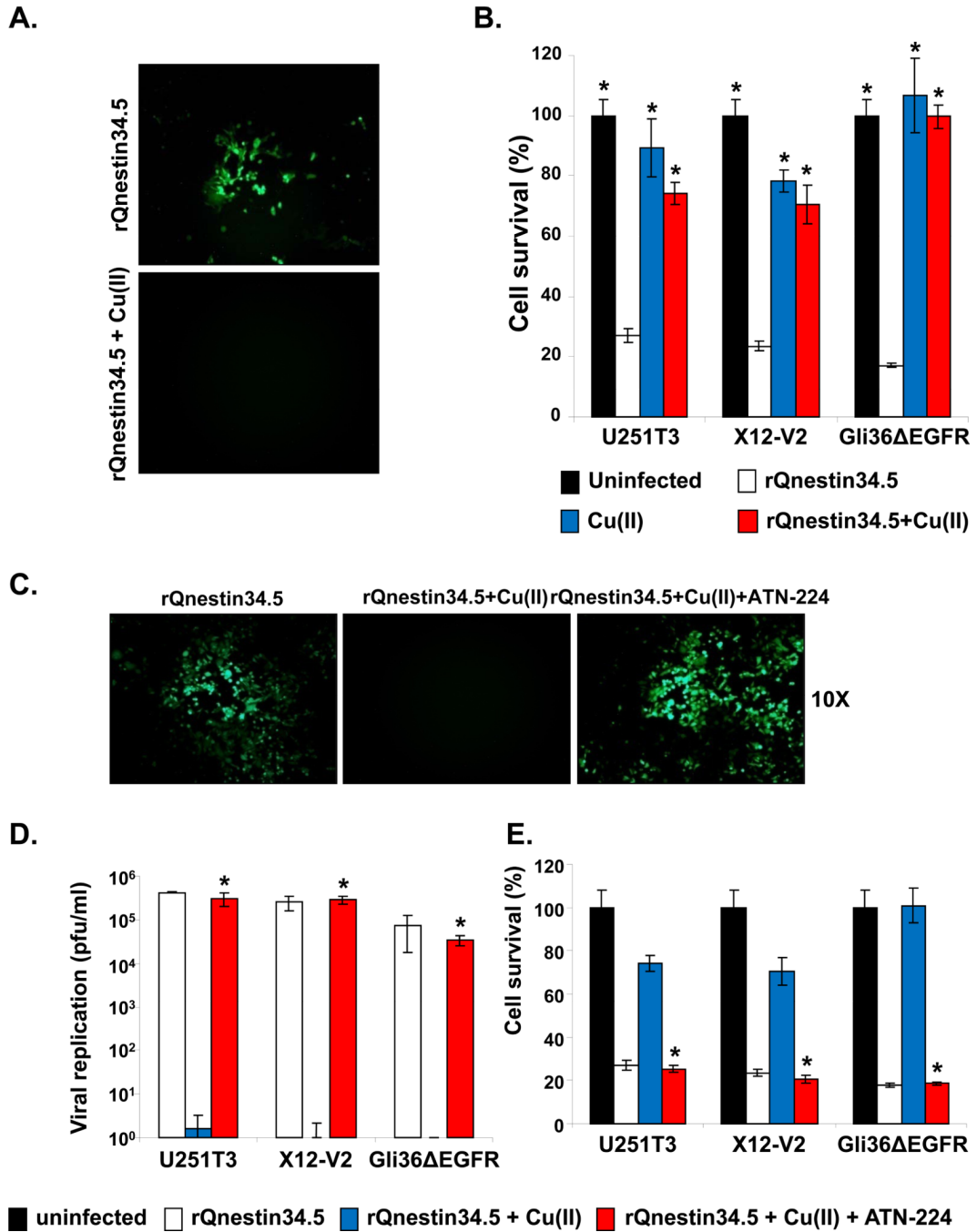


Figure 5. Inhibition of oHSV efficacy by Copper and its rescue with ATN-224

Glioma cells were infected with rQnestin34.5 (MOI=0.1) and incubated with buffer ± Copper (1 mg/L). A) Fluorescence microscopic images of GFP positive Gli36 EGFR glioma cells. B) Percent cell survival of U251T3, X12-V2, and Gli36 EGFR was measured 48 hrs post infection with rQnestin34.5 incubated with or without copper by standard crystal violet assay. *: $P < 0.05$ compared to rQnestin34.5. C–E): ATN-224 rescues copper-mediated inhibition of oHSV infection, replication and glioma cell killing. C) Fluorescent microscopy images of GFP positive Gli36 EGFR glioma cells infected with rQnestin34.5 incubated with Copper ± ATN-224. D) Viral titers were measured in cells infected with rQnestin34.5 pre-incubated with or without Copper ± ATN-224, 48 hrs post infection. *: $P <$

0.05 compared to rQnestin34.5 + Copper. E) Survival of cells infected with rQnestin34.5 pre-incubated with or without Copper \pm ATN-224, 48 hrs post infection. *: $P < 0.05$ compared to rQnestin34.5 + Copper.

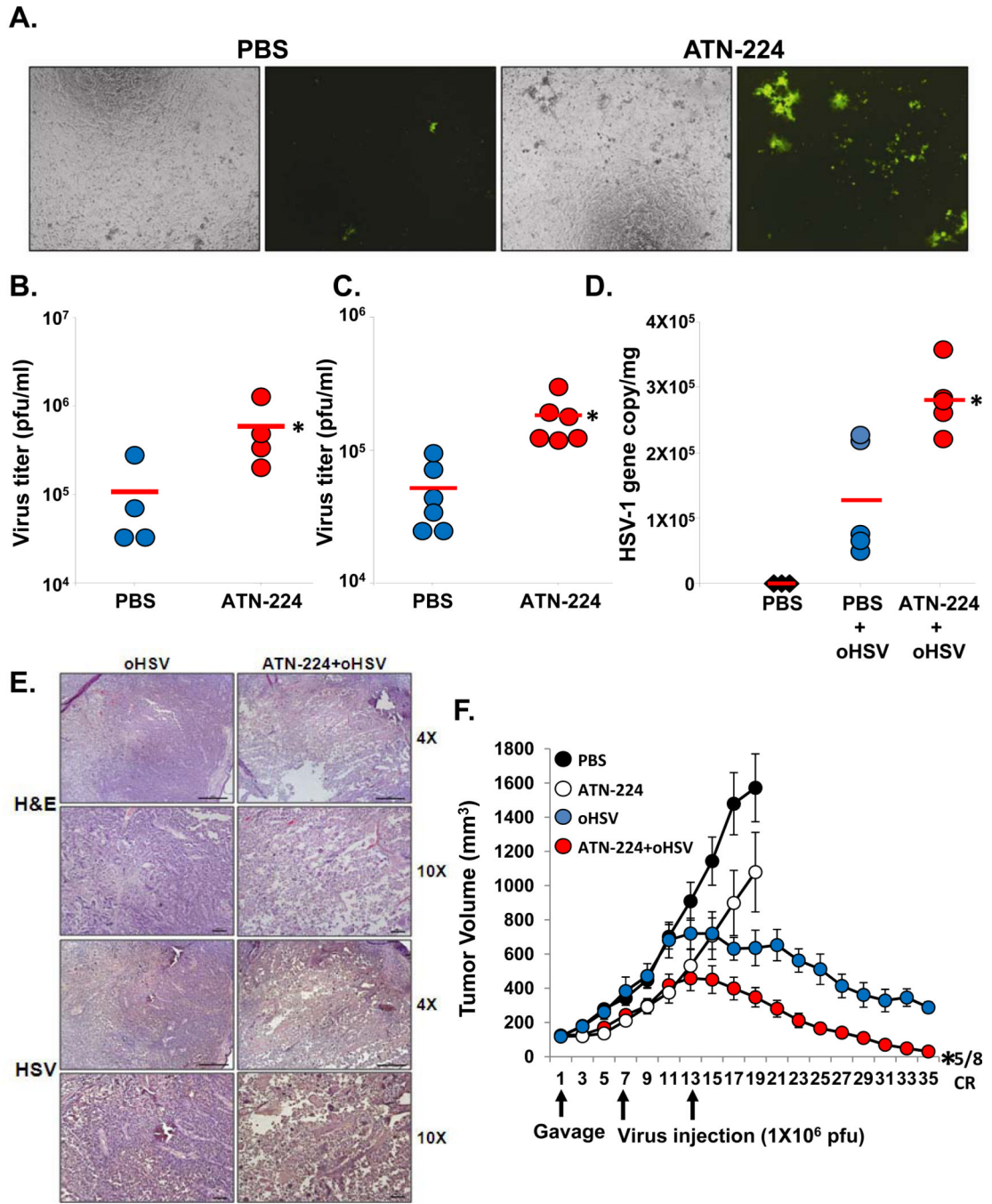


Figure 6. Increased oHSV viability (stability) in ATN-224 treated mice serum

A–B) Ex vivo serum rescue assay. Serum from mice fed PBS or ATN-224 was collected and incubated with rQnestin34.5 for 1 hour at 37 °C (n=4/group). A) Fluorescent microscopy images of GFP positive cells infected with rQnestin34.5 incubated with serum from animals fed PBS or ATN-224. B) Quantification of infectious viral plaque forming units after incubation with serum from mice fed PBS or ATN-224. Data shown are the mean viral titers obtained ± SD (n=4/group). *: *P* < 0.05 compared to PBS. C) Tumor bearing mice fed PBS or ATN-224 by daily gavage, were administered oHSV (hrR3) via tail vein injection. Total virus in serum was measured by a standard plaque assay. Data shown are the mean pfu/ml in serum of mice ± SD (n=6/group). *: *P* < 0.05 compared to PBS. D) ATN-224 treatment

increased systemic delivery of oHSV. Mice with subcutaneous U251T3 tumors were fed PBS or ATN-224 by daily gavage. hrR3 was administered i.v. and tumors were analyzed for viral gene copy. Data shown are mean HSV-1 gene copy/mg of tumor DNA \pm SE. *: $P < 0.05$ compared to PBS. E) Representative photomicrographs of tumor sections stained with anti-HSV-1 antibody highlighting virus propagation in vivo. F) Antitumor efficacy of oHSV is increased in mice bearing subcutaneous U251T3 tumors fed ATN-224 compared to PBS. *: $P < 0.05$ compared to oHSV.